

# Heavy Ion Test Report for the RH5596

Dakai Chen, Andy Mo, and Tom Decker

Test Date:  
TAMU: May 5<sup>th</sup>, 2018  
LBNL: September 11<sup>th</sup>, 2018

## I. Introduction

The purpose of this test was to determine the heavy ion-induced single-event effect (SEE) susceptibility of the RH5596 from Analog Devices.

## II. Device Under Test

The RH5596 is a RMS (root mean square) power detector with wide RF input bandwidth from 100 MHz to 40 GHz. The device is suitable for a wide range of RF and microwave applications. The device is built on a 0.18  $\mu\text{m}$  SiGe BiCMOS process. Figure 1 shows the pin configuration for the DFN package. Table I shows the basic part and test details. The datasheet for the commercial product can be found online [1].

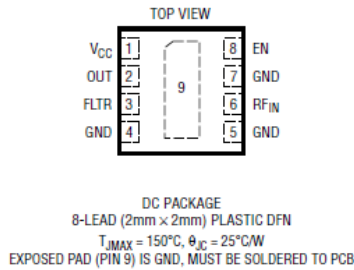


Figure 1. Schematic of the pin configuration.

Table I  
Part and test information.

<b>Part Number:</b>	LTC5596
<b>Manufacturer:</b>	Analog Devices
<b>Package Style:</b>	8-lead DFN flip-chip 16-lead Hermetic LSH6
<b>Quantity Tested:</b>	3
<b>Lot date code:</b>	1401 (DFN) 1823 (LSH6)
<b>Part Function:</b>	Power detector
<b>Part Technology:</b>	0.18 $\mu\text{m}$ SiGe BiCMOS
<b>Test Equipment:</b>	Hittite HMC-T2220 signal generator (SN: TBD) Agilent DSO6034A oscilloscope (SN: MY44002742) Power supply, and Laptop

### III. Test Facility

The heavy-ion beam testing were carried out at the Texas A&M University (TAMU) Cyclotron Facility and the Lawrence Berkeley National Laboratory (LBNL) Berkeley Accelerator Space Effects (BASE) Facility [2], [3]. The TAMU Cyclotron Facility utilizes the K500 cyclotron with a superconducting magnet which generates the magnetic field used to accelerate the ions. The test setup was in an air environment at TAMU. The BASE facility utilizes an 88-inch cyclotron, and the irradiation was carried out in vacuum.

<b>Facility:</b>	TAMU and LBNL
<b>Beam Energy:</b>	15 MeV/amu (TAMU) and 10 MeV/amu (LBNL)
<b>Flux:</b>	$1 \times 10^3$ to $1 \times 10^5$ $\text{cm}^{-2} \cdot \text{s}^{-1}$
<b>Fluence:</b>	up to $1 \times 10^7$ $\text{cm}^{-2}$ (per run)
<b>Ions:</b>	Table II shows the ions used at both facilities

TABLE II  
HEAVY-ION SPECIE, LET, RANGE, AND ENERGY  
15 MeV BEAM AT TAMU.

Ion	Initial LET in air (MeV·cm <sup>2</sup> /mg)	Range in Si ( $\mu\text{m}$ )	Energy (MeV)
Ne	2.6	316	300
Ar	8.0	229	599
Cu	18.7	172	944
Xe	58.8	90	1956

TABLE III  
HEAVY-ION SPECIE, LET, RANGE, AND ENERGY  
10 MeV BEAM AT LBNL.

Ion	LET (MeV·cm <sup>2</sup> /mg)	Range in Si ( $\mu\text{m}$ )	Energy (MeV)
Ar	9.7	130	400
Cu	21.2	108	659
Xe	58.8	90	1233

### IV. Test Method

#### A. Test Setup

The device under test (DUT) was configured according to the 2158A demonstration circuit [3]. Figure 2 shows a schematic of the test setup. Figure 3 shows a schematic diagram of the test circuit. The  $V_{cc}$  and Enable pin were tied together and connected to a 3.3 V supply. The input was fed by a signal generator. The output was connected to an oscilloscope. A custom Python script automated the transient capture process. The applied trigger levels for the oscilloscope accounted for the background noise level at the facilities. Figure 4 show schematic diagrams of the setup at TAMU. The test setup at

LBNL was similar but situated inside a vacuum chamber. The user control rooms are located above the beam chambers at both facilities. The DUT and all necessary equipment (e.g. power supply, signal generator, oscilloscope) were located in the cave. The equipment were interfaced to the user PCs using USB and extension cables routed to the control room via a cable-drop. Figure 5 – 7 shows photographs of the setup at LBNL.

## TEST SETUP

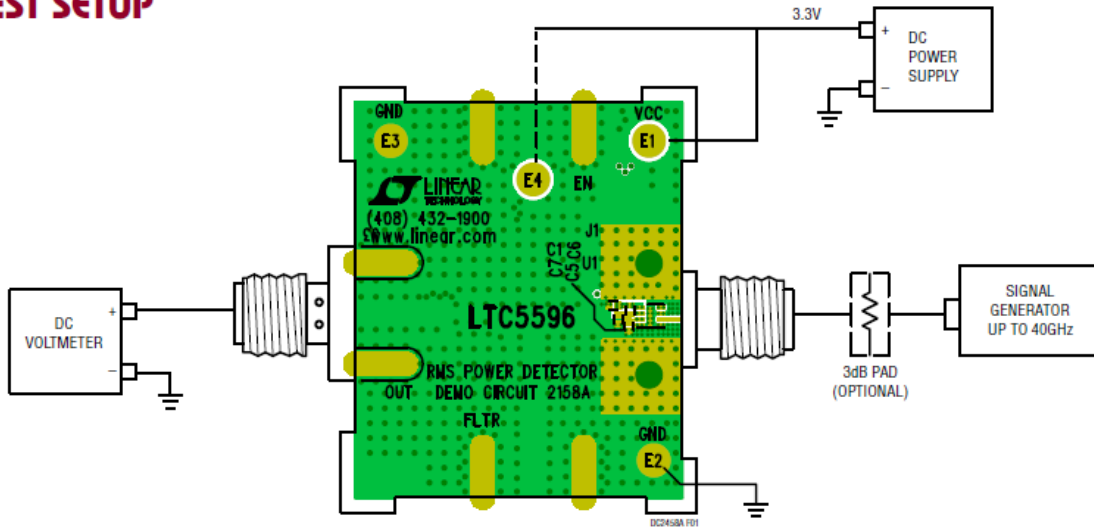


Figure 1: Test Setup for RF Performance Measurements

Figure 2. Schematic drawing of the demonstration board and test setup.

## TEST CIRCUIT

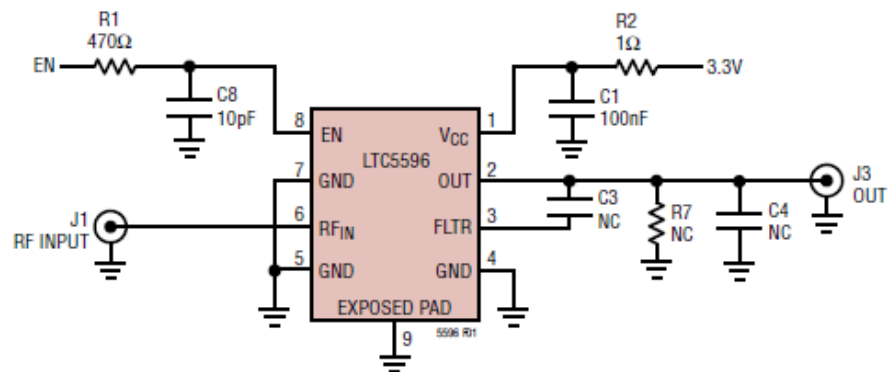


Figure 3. Schematic of the test circuit.

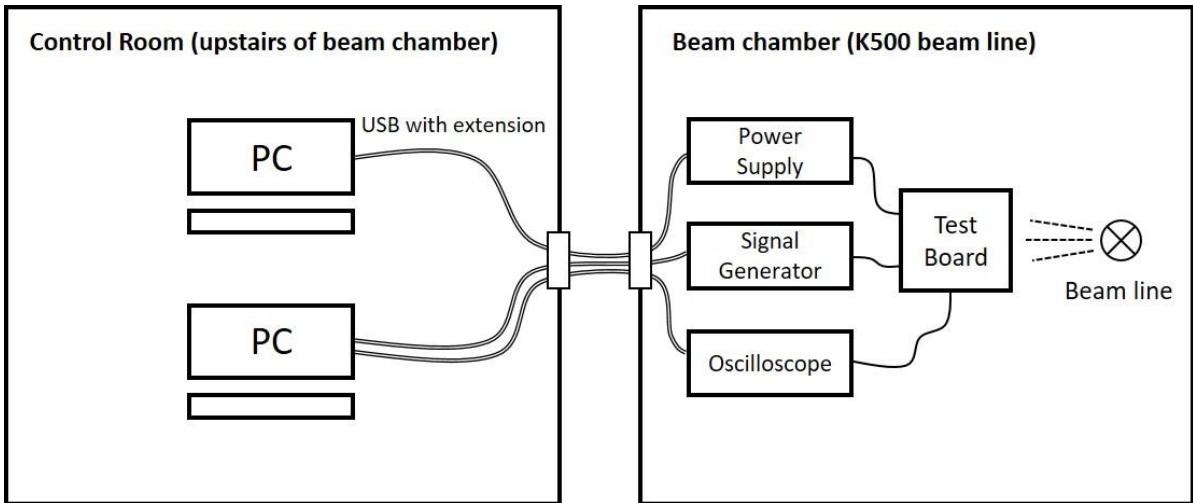


Figure 4. Schematic diagram of the test setup at TAMU.

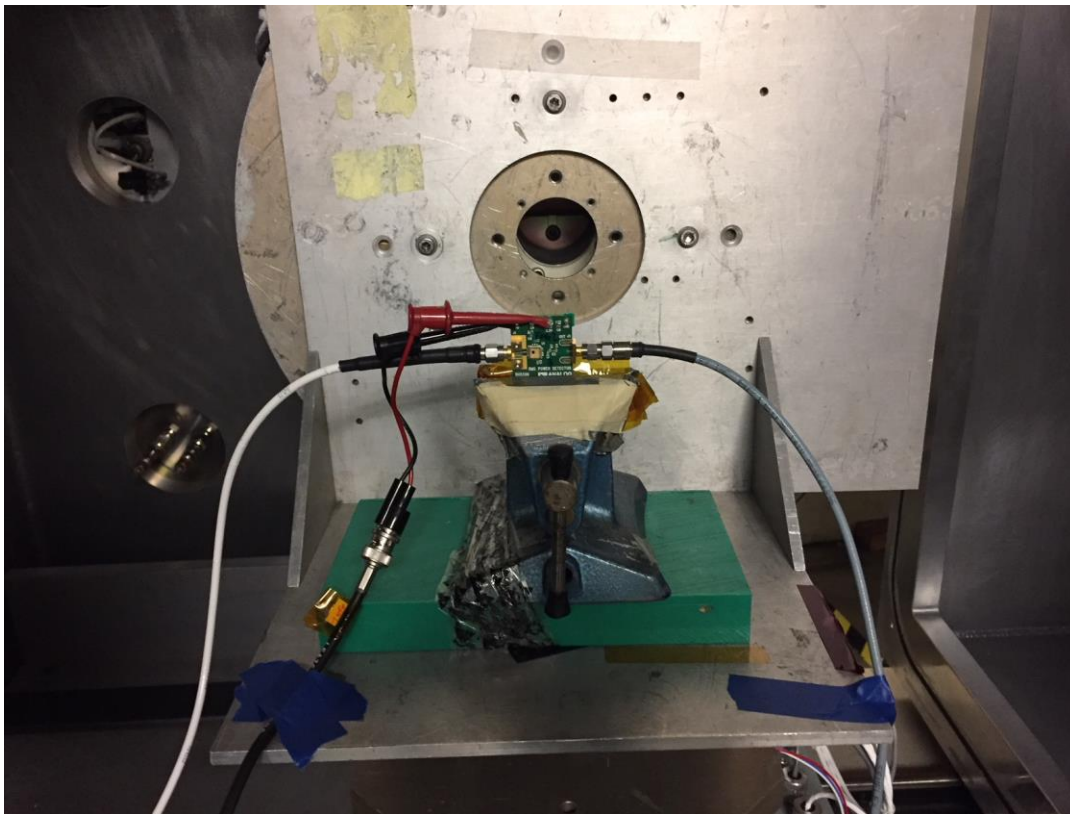


Figure 5. Photograph of the RH5596 test setup at LBNL.

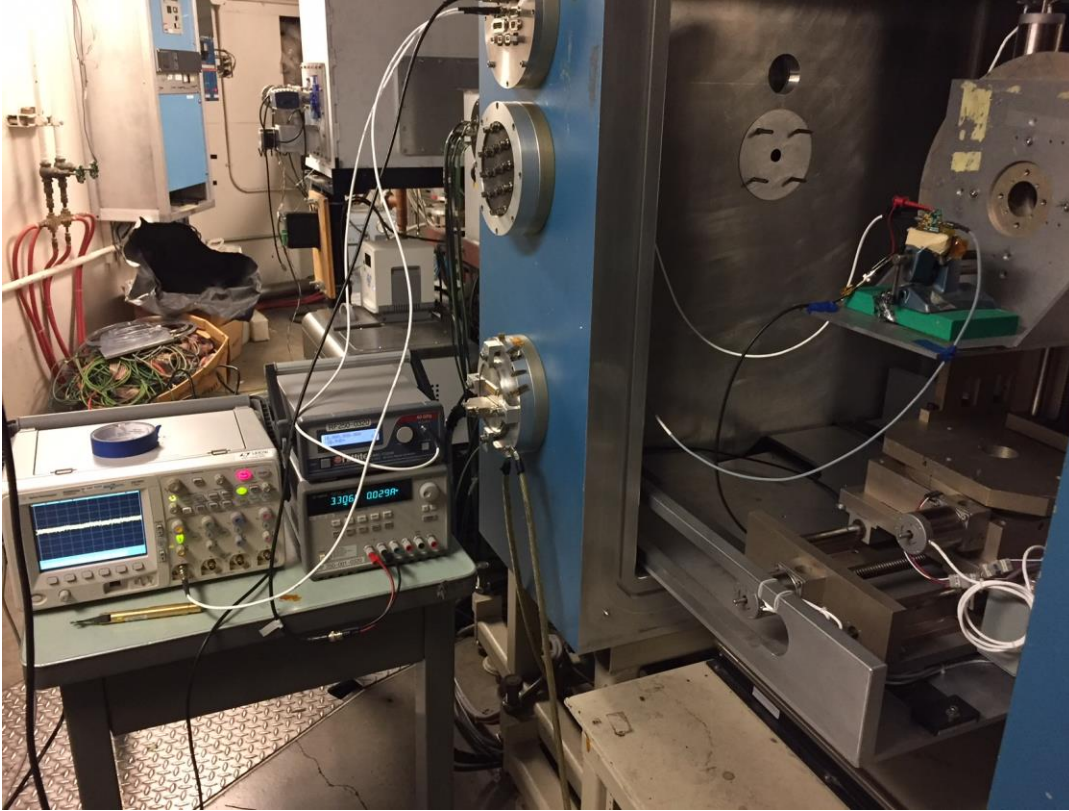


Figure 6. Photograph of the RH5596 test setup at LBNL.

### *B. Irradiation procedure*

The first test at TAMU was carried out for flip-chip packaged devices. The DUTs were prepared for the irradiation by chemically etching away the package top-side to expose the device substrate. Then, the substrate was milled down to a total die thickness of  $\sim 70 \mu\text{m}$  to accommodate the range of 15 MeV/amu heavy ions.

The DUTs used at the LBNL test were packaged in a LSH6 hermetic surface mount package with the die facing up. The lids were taken off for the irradiation. The range of the 10 MeV/amu heavy ions were sufficient to fully penetrate the die.

The test procedures followed JESD57A Test Procedures for the Measurement of Single-event Effects in Semiconductor Devices from Heavy Ion Irradiation [4].

### *C. Test Conditions*

<b>Test Temperature:</b>	Ambient temperature
<b>Operating Frequency:</b>	100 MHz to 40 GHz
<b>Power Supply:</b>	3.3 V (nominal), 2.7 V (minimum), 3.6 V (maximum)
<b>Supply current:</b>	30 mA (nominal), 25 mA (minimum), 35 mA (maximum)
<b>Input Power:</b>	Approximately -32 dBm to 2.9 dBm (at 40 GHz)
<b>Parameters to record:</b>	1) Supply current 2) Output voltage

## V. Results

The device was robust against any destructive or high current event for the applied test conditions, up to an effective LET of  $83.2 \text{ MeV}\cdot\text{cm}^2/\text{mg}$ . The device was vulnerable to single-event transient (SET). Figure 7 shows the SET device cross section as a function of effective LET. The figure includes both TAMU and LBNL data, and a Weibull fit. The data from the two facilities are generally consistent with each other. Notably, we observed some enhancement in the cross section for  $60^\circ$  incident angle irradiations. The data taken at  $60^\circ$  tilt angle are identified in Figure 7. The cross section enhancement is visible for effective LETs of  $4.8 \text{ MeV}\cdot\text{cm}^2/\text{mg}$  (Ne  $60^\circ$ ) and  $15.2 \text{ MeV}\cdot\text{cm}^2/\text{mg}$  (Ar  $60^\circ$ ) from the TAMU data, and is substantial for an effective LET of  $19.5 \text{ MeV}\cdot\text{cm}^2/\text{mg}$  (Ar  $60^\circ$ ) from the LBNL data. On the other hand, there is minimal enhancement in the cross section at an effective LET of  $42.2 \text{ MeV}\cdot\text{cm}^2/\text{mg}$  for irradiation with Cu at LBNL.

We observed minimal change in the SET cross section over a frequency range from 100 MHz to 40 GHz, as shown in Figure 8. However, the SET cross section showed sizeable change over the input power, as illustrated in Fig. 9. The lowest frequency range showed the highest sensitivity to SET. The SET characteristics also varied depending on the power level. Fig. 10 shows a histogram of SET magnitudes. The SETs at a lower power level of -10 dBm showed a much wider range of magnitudes from -0.5 V to 0.8 V, relative to the spectrum of SET magnitudes at a higher power of 10 dBm.

Figure 12 and 13 shows the scatter plot of SET amplitude vs. width captured at TAMU and LBNL, respectively. The SET width is determined at the full-width-half-maximum (FWHM) value. We examined both positive and negative trigger levels with respect to the signal output, and found that the majority of SETs were positive-going. Therefore, the majority of the irradiation runs were carried out with a positive trigger. Figure 12 and 13 also show that the SETs at lower LETs generally have smaller amplitudes than those at higher LETs. In addition, the TAMU test showed a collection of SETs with width between 100  $\mu\text{sec}$  to 1 sec. These SETs are not observed for the LBNL test. The irradiations at TAMU were carried out for a range of LETs from 2.4 to  $46 \text{ MeV}\cdot\text{cm}^2/\text{mg}$ , whereas at LBNL the range of LETs varied from 9.7 to  $83.2 \text{ MeV}\cdot\text{cm}^2/\text{mg}$ . The predominate number SETs with width between 100  $\mu\text{sec}$  to 1 sec have small amplitudes obtained at relatively lower LETs. The LBNL test did not include the lower range LETs. So, those longer duration and short amplitude SETs were not observed at LBNL. Fig. 13 shows an example of a SET at a LET of  $46.3 \text{ MeV}\cdot\text{cm}^2/\text{mg}$ . Figure 14 shows waveforms of all the SETs captured during an irradiation run at a LET of  $46.3 \text{ MeV}\cdot\text{cm}^2/\text{mg}$ , with frequency of 100 MHz and input power of -10 dBm.

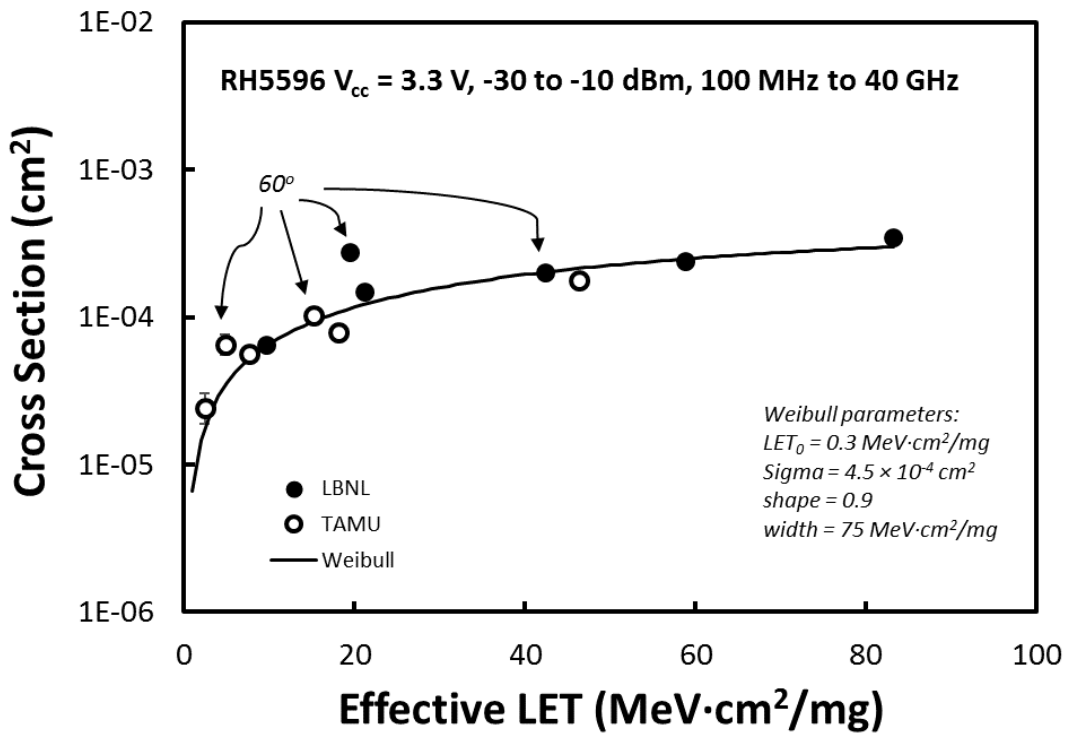


Figure 7. SET cross section vs. effective LET for the RH5596 irradiated at LBNL and TAMU.

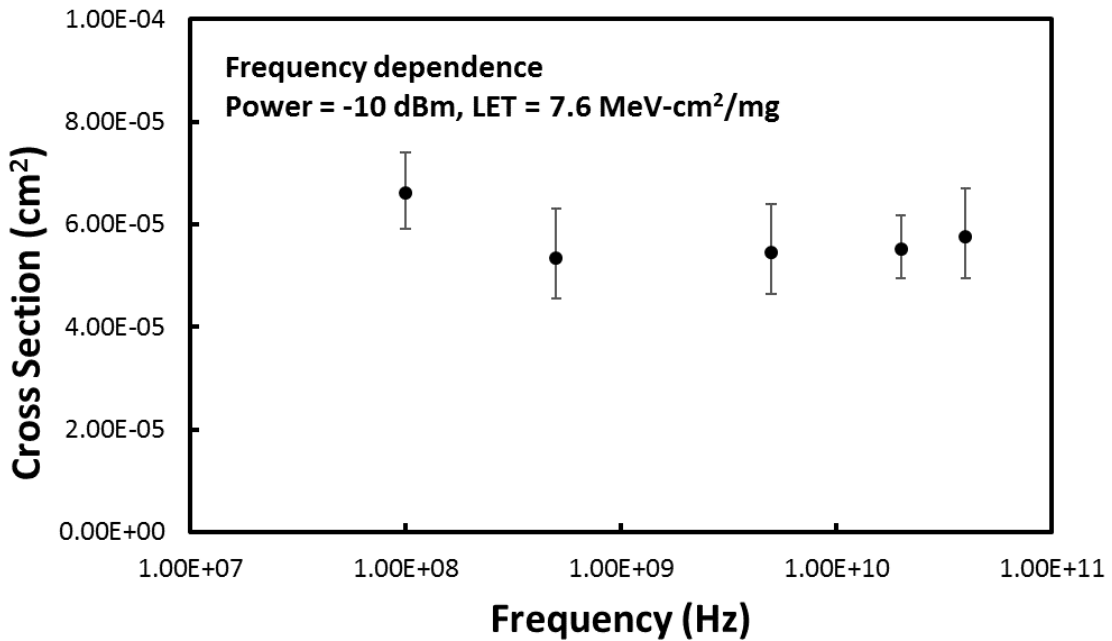


Figure 8. SET cross section vs. frequency for the RH5596 with input power of -10 dBm and an effective LET of 7.6 MeV·cm<sup>2</sup>/mg.

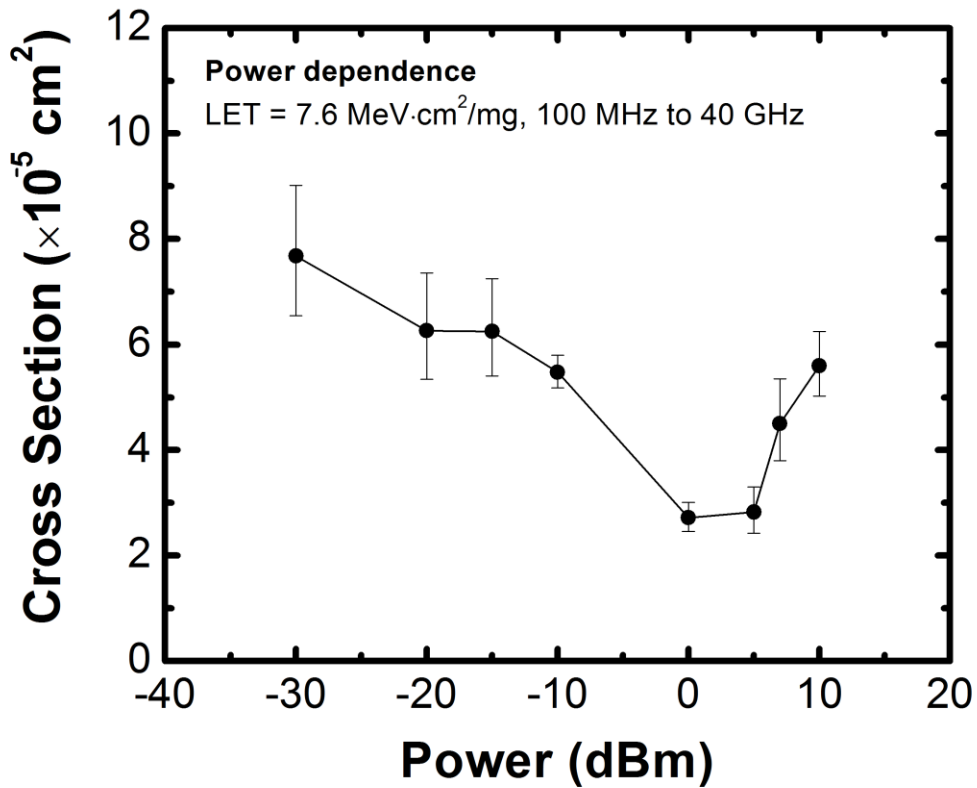


Figure 9. SET cross section vs. input power for the RH5596 irradiated with frequency of 100 MHz to 40 GHz and an effective LET of 7.6 MeV·cm<sup>2</sup>/mg.

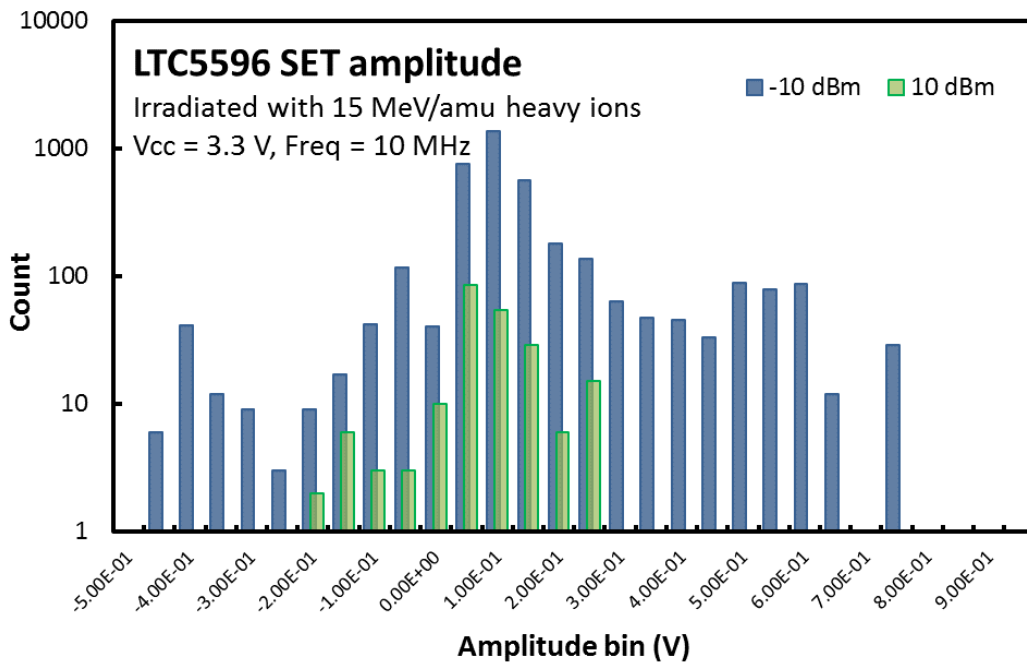


Fig. 10. Histogram of SET amplitude for the RH5596 irradiated with input power of -10 and 10 dBm.

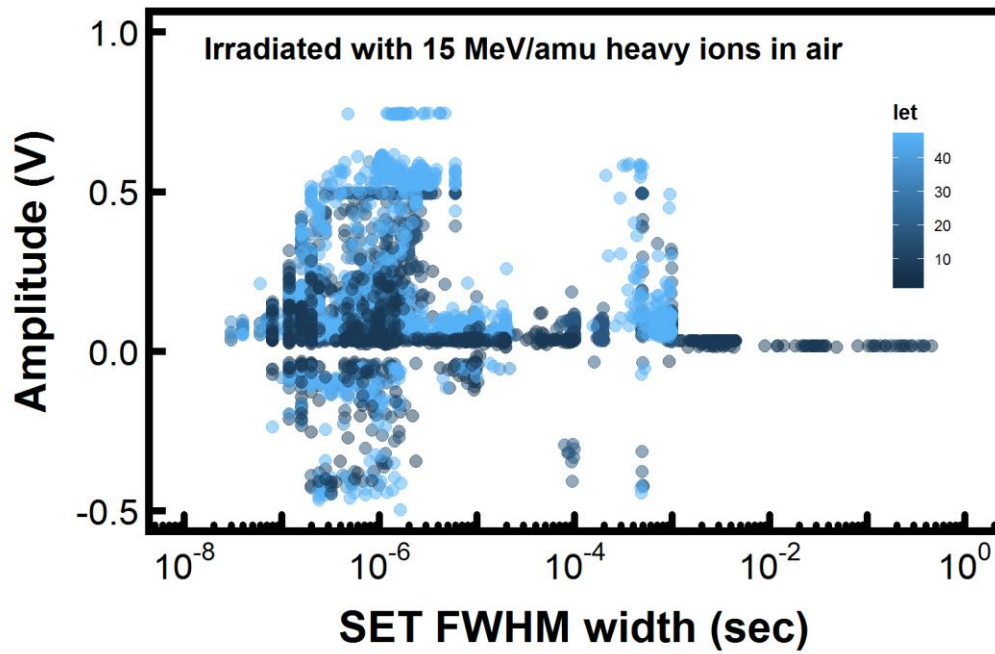


Fig. 11. SET scatter plot of amplitude vs. width for the RH5596 irradiated at TAMU with 15 MeV/amu heavy ions in air.

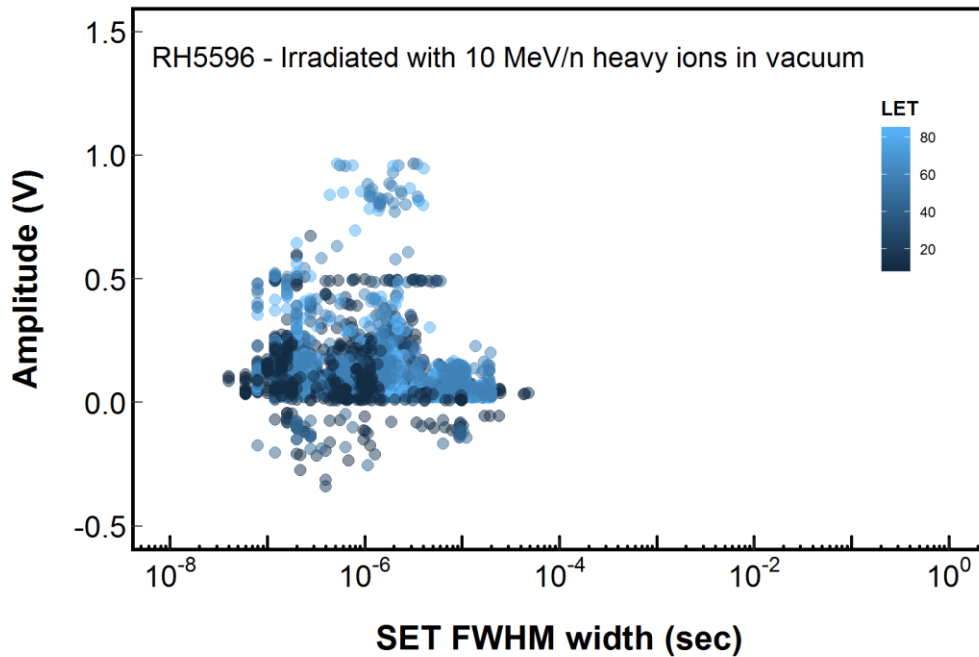


Fig. 12. SET scatter plot of amplitude vs. width for the RH5596 irradiated at LBNL with 10 MeV/amu heavy ions in vacuum.

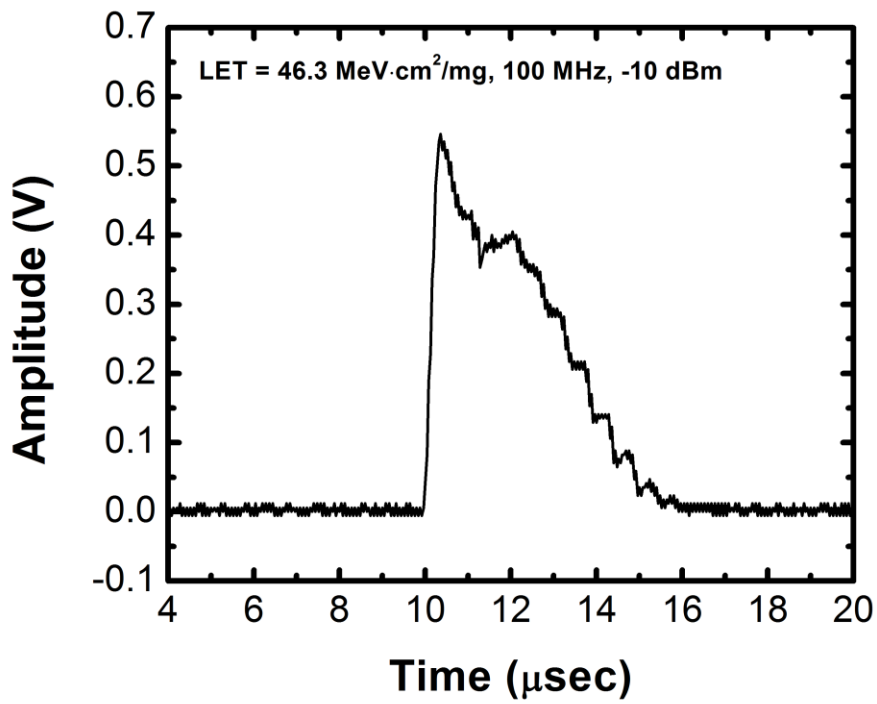


Fig. 13. SET characteristics for irradiation with Xe at a LET of 46.3 MeV·cm<sup>2</sup>/mg, and device operating frequency of 100 MHz and input power of -10 dBm.

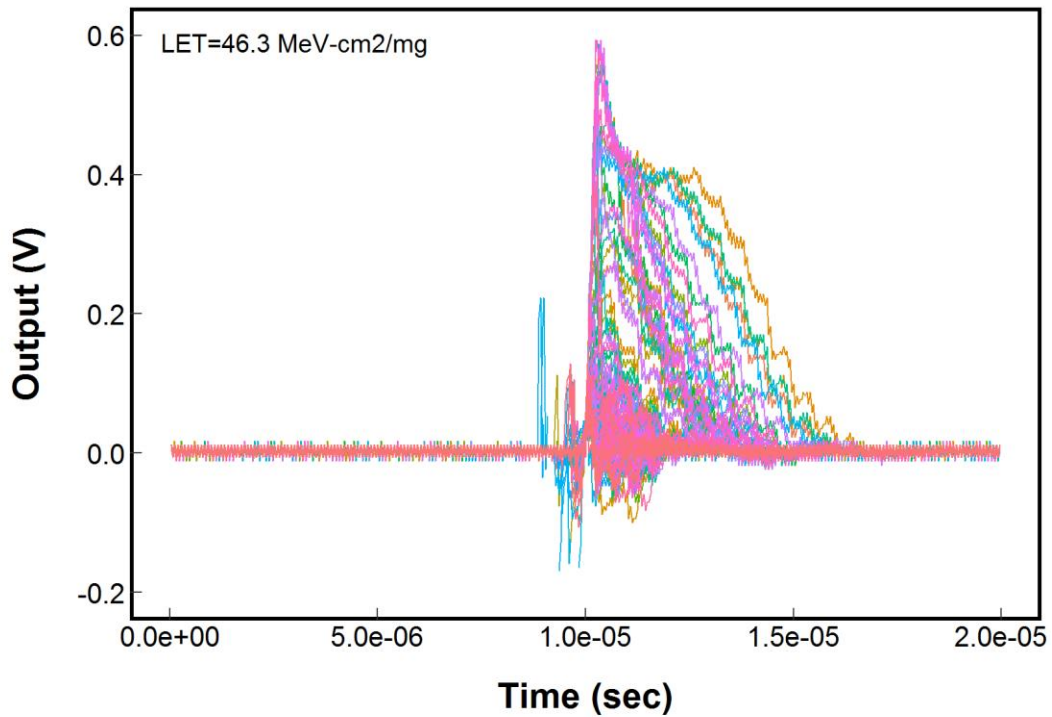


Fig. 14. A collection of SETs for an irradiation run with Xe at a LET of 46.3 MeV·cm<sup>2</sup>/mg, and device operating frequency of 100 MHz and input power of -10 dBm.

## VI. Conclusion

We found that the RH5596 was robust against destructive or high current event for the applied test conditions up to an effective LET of  $83.2 \text{ MeV}\cdot\text{cm}^2/\text{mg}$ . The device is susceptible to SET. The SET device cross section was relatively insensitive across the operating frequency. The cross section increased with decreasing input power for less than 0 dBm. The cross section showed a minimum value at 0 dBm, then increased for increasing input power for values greater than 0 dBm. The SET amplitudes increased with increasing LET in general. The SETs were predominately positive-going.

## VII. Reference

1. Analog Devices, Inc. (2017) "*LTC5596 - 100MHz to 40GHz Linear-in-dB RMS Power Detector with 35dB Dynamic Range*" [Online]. Available: <http://www.analog.com/en/products/amplifiers/rf-power-detectors/rms-responding-power-detectors/ltc5596.html>, Accessed on: April 10, 2018.
2. B. Hyman, "Texas A&M University Cyclotron Institute, K500 Superconducting Cyclotron Facility," <http://cyclotron.tamu.edu/facilities.htm>, Jul. 2003.
3. Analog Devices, Inc. (2017) "*DC2158A - LTC5596 Demo Board | 100MHz to 40GHz RMS Power Detector*" [Online]. Available: <http://www.analog.com/en/design-center/evaluation-hardware-and-software/evaluation-boards-kits/dc2158a.html>, Accessed on: April 10, 2018.
4. JEDEC Government Liaison Committee, Test Procedure for the Management of Single-Event Effects in Semiconductor Devices from Heavy Ion Irradiation," JESD57, <http://www.jedec.org/standards-documents/docs/jesd-57>, Dec. 1996.